Available online at www.sciencedirect.com
SCIENCE DIRECT®
Journal of Sound and Vibration 287 (2005) 329–342
JOURNAL OF SOUND AND VIBRATION
www.elsevier.com/locate/jsvi

A numerical study of a dry friction oscillator with parametric and external excitations

Gong Cheng, Jean W. Zu*

Department of Mechanical & Industrial Engineering, University of Toronto, 5 King's College Road, Toronto, Ont., Canada M5S 3G8

Received 26 January 2004; received in revised form 7 October 2004; accepted 4 November 2004
Available online 9 February 2005

Abstract

In this paper, the dynamic behavior of a block-on-belt system subjected to simultaneous parametric and external excitations is studied, in which the parametric excitation arises from the variable stiffness of a spring in the system while the external excitation consists of a harmonic force. In addition, the system is damped by dry friction that follows the classical Coulomb's law. The focus of the paper is on analyzing the influence of the parametric excitation on the qualitative features of system dynamics, under various frequency ratios between the external and parametric excitations. Numerical simulations are carried out, whose results are visualized by means of bifurcation diagrams, Poincaré sections and Lyapunov exponents. The results show that the system possesses rich dynamics characterized by periodic, quasi-periodic and chaotic attractors. Furthermore, it is found that the parametric excitation amplitude and the frequency ratio between the excitations have a significant impact on the dynamical behavior of the system.

1. Introduction

The vibration of dry friction damped systems has been of considerable interest to researchers for a long time, for it occurs frequently in everyday life as well as in engineering systems such as creaking doors, squeaking chalks, and rattling turbine blade joints. In addition, dry friction as a

*Corresponding author. Tel/fax: +1 416 978 0961.
E-mail address: zu@mie.utoronto.ca (J.W. Zu).

0022-460X/$ - see front matter © 2005 Elsevier Ltd. All rights reserved.
doi:10.1016/j.jsv.2004.11.003

discontinuous nonlinearity poses challenges to researchers since most results for differentiable systems cannot be directly applied to dry friction-damped systems. Recent research has shown that really complex dynamics, e.g. chaos, can be exhibited from very simple systems under dry friction even in its simplest form, Coulomb damping.

Among the earliest research on dry friction oscillations is that of Den Hartog [1], where an exact solution was presented for the steady-state vibration of an sdof harmonically excited system subjected to dry friction. He also performed several experimental tests to verify his solutions. Since then, a great amount of research has been done in this field, and some of the recent work is summarized as follows. Feeny and Moon [2] investigated the geometry of chaotic attractors for dry friction oscillators experimentally and numerically, using three different friction laws. Later, Oestreich et al. [3] employed a one-dimensional map to discuss bifurcation and stability of a dry friction damped block-on-belt system, and the map approach was shown to be an efficient and illustrative way to carry out such analysis. The response of a dry friction damped block-on-belt system was also analyzed by Andreaus and Casini [4], with emphasis laid on the influence of the belt speed and the friction modeling on the system response. In the paper of Van De Vrande et al. [5], both stable and unstable periodic solutions were derived for the stick-slip vibration of an autonomous dry friction oscillator with a smoothing procedure. The work of Galvanetto [6,7] dealt with dynamics of a three-block mechanical system with dry friction, as well as discontinuous bifurcations in a two-block system affected by dry friction. Most recently, Thomsen and Fidlin [8] considered friction-induced vibrations of a mass-on-belt system, and they obtained approximate analytical expressions for the amplitudes and base frequencies of stick-slip and pure-slip oscillations.

In all of the research above, either no excitation or only a single harmonic excitation was assumed. In practice, however, multiexcitations can exist in various vibration systems with dry friction, and they may have a dramatic effect on the system's dynamic characteristics. To address the lack of research on this issue, the authors [9] studied the vibration of a single-degree-of-freedom dry friction damped system subjected to two harmonic disturbing forces with different frequencies and determined analytically the steady-state responses for the system undergoing periodic pure-slipping and stick-slip motions. Moreover, we extended our study to the rotational vibration of a multidegree-of-freedom belt drive system with a dry friction tensioner subjected to multiple harmonic excitations [10], in which an analytical solution procedure was developed to predict two kinds of periodic responses of the system characterized by the non-stick and stick-slip vibration of the tensioner arm in the system, respectively. In a recent paper [11], we delved into the chaotic aspects of sdof two-frequency oscillations with dry friction. All our previous studies have shown the significant influence of multifrequency excitations combined with dry friction. In this paper, we further our study into a dry friction oscillator subjected to both parametric and external excitations with different frequencies. Multiexcitations can arise also in absence of external harmonic excitations as in the case of the block being dragged by multiple rough belts characterized by different friction parameters and moving with different velocities [12]. With respect to the research on parametric vibrations, some most recent studies are Refs. [13–15]. In the present study, the dynamics of a block-on-belt system subjected to simultaneous parametric and external excitations is investigated, with focus laid on bifurcation analysis to gain insight into the influence of the parametric excitation on the qualitative features of system dynamics. Numerical simulations are carried out, which show that the system possesses rich dynamics characterized by

periodic, quasi-periodic and chaotic attractors. Furthermore, it is found that the parametric excitation amplitude and the frequency ratio of the external and parametric excitations have a significant impact on the dynamical behavior of the system.

2. System description

The investigated system is shown in Fig. 1, where a mass m is connected to a fixed support via a spring of variable stiffness k and is sliding on a moving belt with a constant velocity v_0. The mass is subjected to a harmonic excitation, namely $P\cos\Omega t$, and dry friction as well when there exists relative motion or a tendency towards relative motion between the mass and the belt. In the study, the following assumptions are made:

The spring stiffness varies periodically as

$$k(t) = k_0(1 + \varepsilon\cos\omega t) \tag{1}$$

in which k_0, ε and ω are constants. Furthermore, the excitation frequency is proportional to the frequency of the spring stiffness

$$\frac{\Omega}{\omega} \equiv v = \frac{M}{N}, \tag{2}$$

where M and N are incommensurable integers.

The dry friction between the mass and the belt follows Coulomb's friction law characterized by a static friction coefficient μ_s and a smaller kinetic friction coefficient μ_k.

The equation of motion for the oscillator is given by

$$m\ddot{x} + k_0(1 + \varepsilon\cos\omega t)x = P\cos\Omega t - \mu N\,\mathrm{sgn}(\dot{x} - v_0), \tag{3}$$

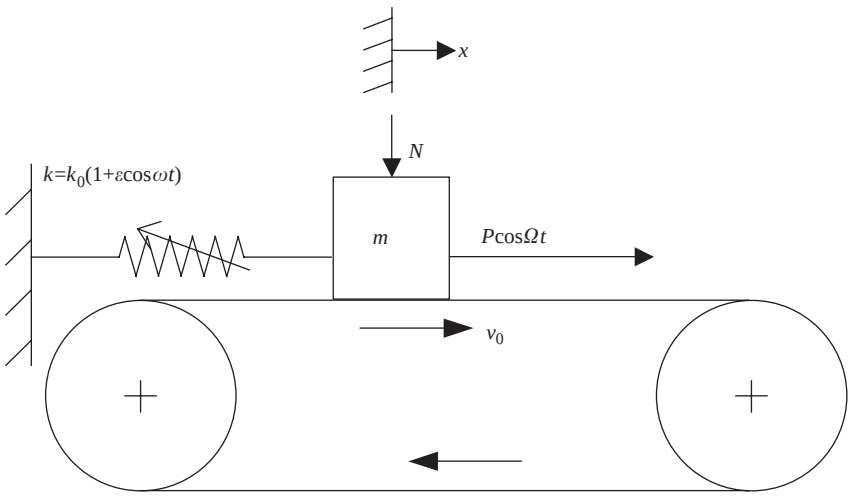

Fig. 1. Model of a dry friction oscillator.

where x denotes the displacement of the mass, N is the normal force in the contact area, and

$$\mu = \begin{cases} \mu_k & (\dot{x} \neq v_0), \\ \mu_s & (\dot{x} = v_0), \end{cases} \tag{4}$$

$$\operatorname{sgn}(y) \begin{cases} = 1 & (y > 0), \\ \in [-1, 1] & (y = 0) \quad y \in \mathbf{R}, \\ = -1 & (y < 0). \end{cases} \tag{5}$$

By defining the quantities

$$\omega_n = \sqrt{\frac{k_0}{m}}, \quad \tau = \omega_n t, \quad \eta = \frac{\omega}{\omega_n}, \quad x_v = \frac{v_0}{\omega_n}, \quad x_p = \frac{P}{k_0},$$
$$x_f = \frac{\mu N}{k_0} = \begin{cases} x_{fk} & (\dot{x} \neq v_0), \\ x_{fs} & (\dot{x} = v_0). \end{cases} \tag{6}$$

Eq. (3) can be normalized as

$$x'' + x + \varepsilon x \cos \eta\tau = x_p \cos \nu\eta\tau - x_f \operatorname{sgn}(x' - x_v) \tag{7}$$

in which the prime indicates differentiation with respect to the non-dimensional time τ.

3. Dynamic analysis

3.1. Computational technique for solutions

For the system described by Eq. (7), two types of steady motion are possible: one is the non-stick motion in which the mass never or only instantaneously reaches the speed of the moving belt, and the other is the stick-slip motion in which the mass slips on and sticks to the belt alternately. To determine which type of steady motion the system enters, we need to compute its time history using the following technique. In general, the mass may experience both the slip mode ($x' \neq x_v$) and the stick mode ($x' = x_v$), given an arbitrary initial condition. For the slip mode, a fourth-order Runge–Kutta varying-step algorithm can be adopted to solve the differential Eq. (7) with sufficient precision; while for the stick mode, the mass simply moves with the velocity of the moving belt. The main computational error, however, arises from the detection of transitions from one mode of motion to another. Hence, the computation of the precise time value when the transition occurs is of crucial importance to the accuracy of the results. The general idea of our approach is to judge if the mode of motion changes after one time step. Two types of time steps are used: one is fixed while the other is variable. The fixed non-dimensional time step is set to be 0.01 to ensure that no mode of motion is omitted in the calculation, while the varying one is decreased by half consecutively to make sure that the value of the transition time is precise to the order of 10^{-16}, and thereby the accuracy of the results can be guaranteed. In the procedure, a function is constructed with a return value showing which mode of motion the system state lies in, and the corresponding solution subroutine is then utilized to move the system state continuously

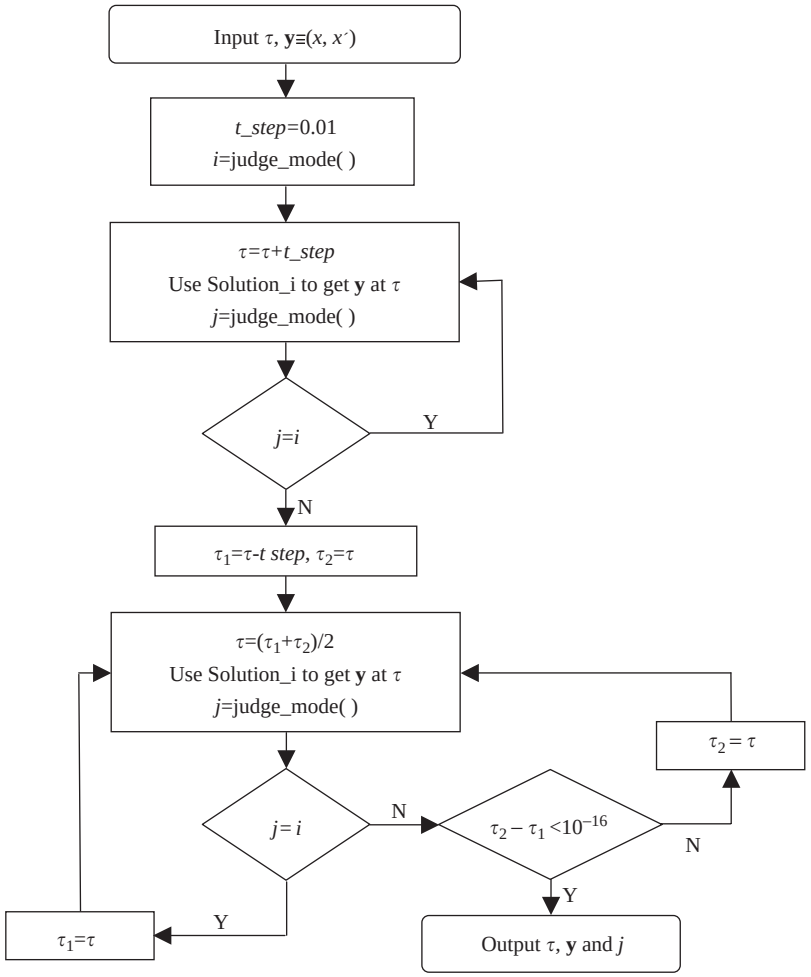

Fig. 2. Flow chart for detecting transitions.

forward by the fixed time step until the mode of motion changes. Then, we move the system state one fixed time step backward, and evolve it with varying time steps till we obtain the transition time with satisfactory precision. To illustrate this procedure, a flow chart is shown schematically in Fig. 2. It is noted that the function of "judge_mode ( )" in the flow chart is based on the speed relationship between the mass and the belt, as well as on the magnitude relationship between the static dry friction and other forces applied on the mass when its speed is equal to the belt speed.

3.2. Poincaré section, bifurcation diagram and Lyapunov exponent

In the above section, we have developed a computational technique with which the time history of the system can be determined under any initial conditions. Although time history by itself can hardly reveal any qualitative features of the system dynamics, it provides a foundation for the

study of the system's qualitative dynamic behavior, which will be discussed in this section from the perspectives of Poincaré sections, bifurcation diagrams and Lyapunov exponents.

In Eq. (7), the periods of the two functions in time, i.e. $\cos \eta\tau$ and $\cos \nu\eta\tau$, are proportional to each other due to the fact that ν is a ratio of two integers M and N as in Eq. (2). Thus, these two functions have a common factor circular frequency

$$\omega^* = \frac{\eta}{N}, \tag{8}$$

which renders it possible to construct a three-dimensional phase space to study the dynamics of the system. By introducing the phase angle

$$\varphi \equiv \omega^*\tau \mod 2\pi \in [0, 2\pi), \tag{9}$$

a phase space can be defined in cylindrical coordinates (r, θ, z) as

$$r = x, \quad \theta = \varphi, \quad z = x'. \tag{10}$$

In the above phase space, two-dimensional Poincaré sections can also be established:

$$\{(x, x')|\varphi = \varphi_0 \in [0, 2\pi)\}, \tag{11}$$

where φ_0 is an arbitrary constant. As is well known, Poincaré sections are very useful in distinguishing different types of motion: periodic, quasi-periodic or chaotic.

For dry friction damped systems, another powerful tool is the mapping method. A map is a relationship which links one point in the state space to another, and its obvious advantage is the reduction of the dimension of the system. Naturally, one can choose stick-to-slip transition states as mapping points as they correspond to the discontinuity of dry friction. Let x_n be the nth stick-to-slip displacement of the mass and φ_n be its corresponding phase angle as defined in Eq. (9). The following relationship between x_n and φ_n can be derived:

$$x_n = \frac{x_p \cos(M\varphi_n) \pm x_{fs}}{1 + \varepsilon \cos(N\varphi_n)} \tag{12}$$

in which the upper and lower part of the compound sign $\pm$ corresponds to the entered slip mode where $x' < x_v$ and $x' > x_v$, respectively. With x_n, bifurcation diagrams can be drawn on which post-transient points of x_n vs. the value of bifurcation parameters are plotted, from which the influence of bifurcation parameters on the system dynamics can be analyzed. Based on φ_n, the following one-point map is introduced

$$H : \varphi_n \mapsto H(\varphi_n) = \varphi_{n+1} \quad (n = 1, 2, \ldots), \tag{13}$$

which allows a simple determination of the maximal Lyapunov exponent λ of the system, cf. Ref. [16]:

$$\lambda = \lim_{n\to\infty} \frac{1}{n} \sum_{p=0}^{n-1} \ln |H'(\varphi_p)|. \tag{14}$$

Fig. 3 shows a one-dimensional map with $M = 1, N = 2$ and $\varepsilon = 0.25$, which is discontinuous. Owing to the discontinuity of the map, care must be taken in the computation of the Lyapunov exponent. We use finite difference technique to calculate the derivative in Eq. (14), and make sure that the points used to calculate the derivative are on the same continuous branch of the map. In a

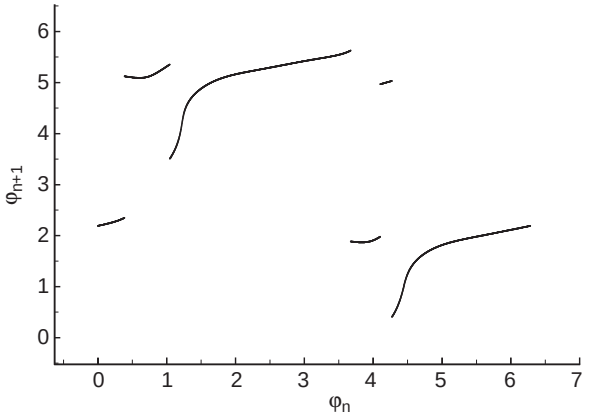

Fig. 3. A one-point map with $M = 1, N = 2, \varepsilon = 0.25$.

repeated process, the difference between $H(\varphi)$ and $H(\varphi + \Delta\varphi)$ is examined, and in case it is 'too large', a smaller $\Delta\varphi$ is chosen until the images become close to each other. Finally, it should be pointed out that the above discussion of the bifurcation diagram, one-dimensional map and Lyapunov exponent is applicable only to the stick-slip motion, which is the major interest of this study. For the case of non-stick motion where the mass never reaches the belt speed, we can define the states of the mass where its velocity equals zero as the mapping points instead.

4. Numerical results

In this section, bifurcation diagrams are plotted to illustrate the influence of the parametric excitation on the dynamic behavior of the system under various external and parametric excitation frequencies. Two system parameters are considered: one is the bifurcation parameter ε, which indicates the amplitude of the parametric excitation, and the other is the ratio between the external and parametric excitation frequencies, namely, M/N. In the simulations, the basic system properties are assumed to take the values

$$p = 0.25, \quad x_{fk} = 2.5, \quad x_{fs} = 4.0, \quad x_v = 1, \quad \eta = \frac{2}{3}. \tag{15}$$

As is well known, in nonlinear systems different attractors can occur corresponding to different initial conditions. Since we do not perform attraction basin analysis in this study, it is pointed out that the following remarks are limited to the attractors shown in the figures. Fig. 4 shows the stick-to-slip transition displacement x as a function of the parameter ε when $M < N$. Only post-transient points are plotted in the figure so that it reflects the steady-state motion of the system. Fig. 4(a) displays the case where M equals 4 and N equals 7. It is observed that for ε starting from 0 up to around 0.21, both non-periodic and periodic responses appear, and they mingle with each other. Furthermore, non-periodic responses occupy the majority of the above parametric range. When the parameter ε becomes larger than 0.21, however, the system exhibits only periodic

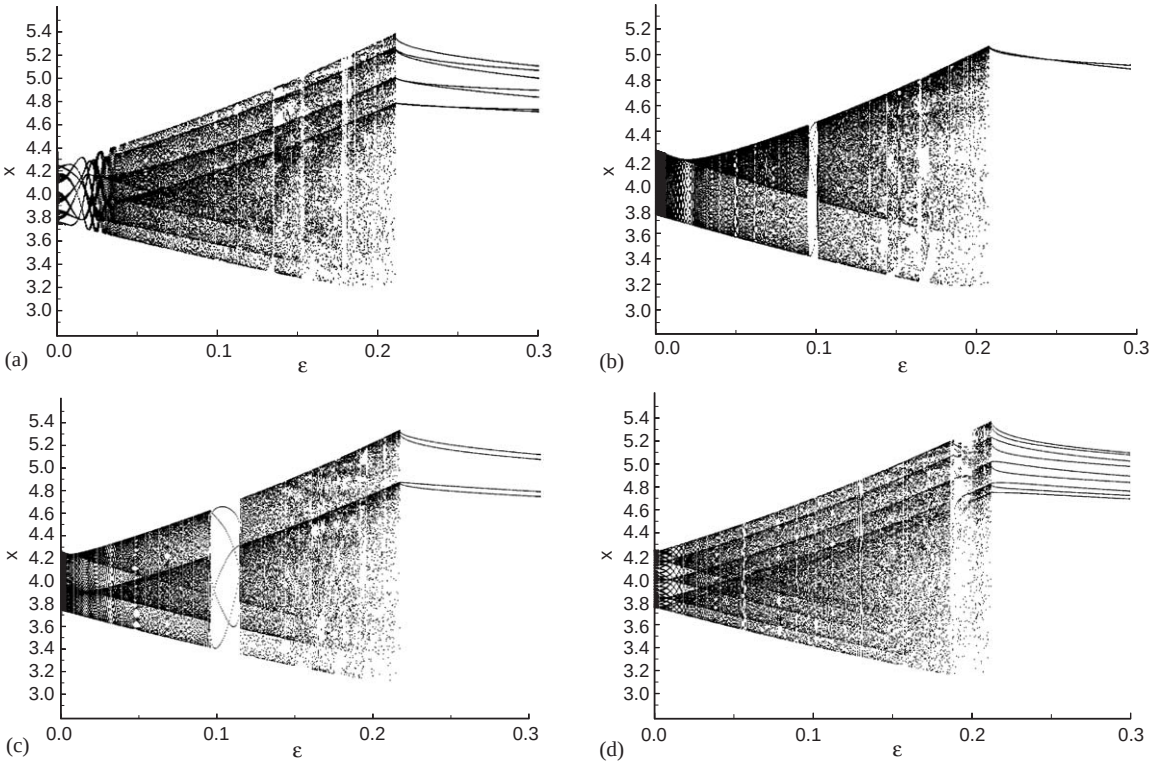

Fig. 4. Transition displacement x vs. ε with $M<N$: (a) $M=4, N=7$; (b) $M=1, N=2$; (c) $M=1, N=4$; (d) $M=1, N=9$.

motion and its periodic number is always 7 regardless of different values of ε. Figs. 4(b)–(d) correspond to the cases of M/N equal to 1/2, 1/4 and 1/9, respectively, in which similar structures are demonstrated in comparison with Fig. 4(a). More interestingly, it is found that only periodic solutions exist when ε exceeds the same critical value, 0.21, despite the variation of the ratio M/N, and the corresponding periodic number is equal to N. Furthermore, the type of the bifurcations at $\varepsilon=0.21$ can be investigated with the aid of the one-dimensional map defined in Eq. (13). To illustrate, consider the case of $M=4$ and $N=7$, as shown in Fig. 4(a). Since the corresponding periodic motion is of 7-period when $\varepsilon$is larger than 0.21, we compute the 7th iterated map, namely, $(7):\varphi_n \mapsto H^{(7)}(\varphi_n)=\varphi_{n+7}$, with three different values of the bifurcation parameter, as displayed in Fig. (5). Fig. 5(a) is for $\varepsilon=0.25$which corresponds to the periodic motion. Evidently, seven stable fixed points occur, indicated by the seven intersection points of the iterated map curve and the straight line $\varphi_{n+7}=\varphi_n$. In Fig. 5(b), one can see that there exists no fixed point for $\varepsilon=0.20$, which is selected from the non-periodic band in the left neighborhood of the bifurcation point. Finally, the case for the bifurcation point $\varepsilon=0.21$ is plotted in Fig. 5(c), where the curve of the iterated map is tangent to the 45° straight line. Thus, we can conclude that a tangent bifurcation gives rise to the transition from the non-periodic motion to the periodic motion of the system.

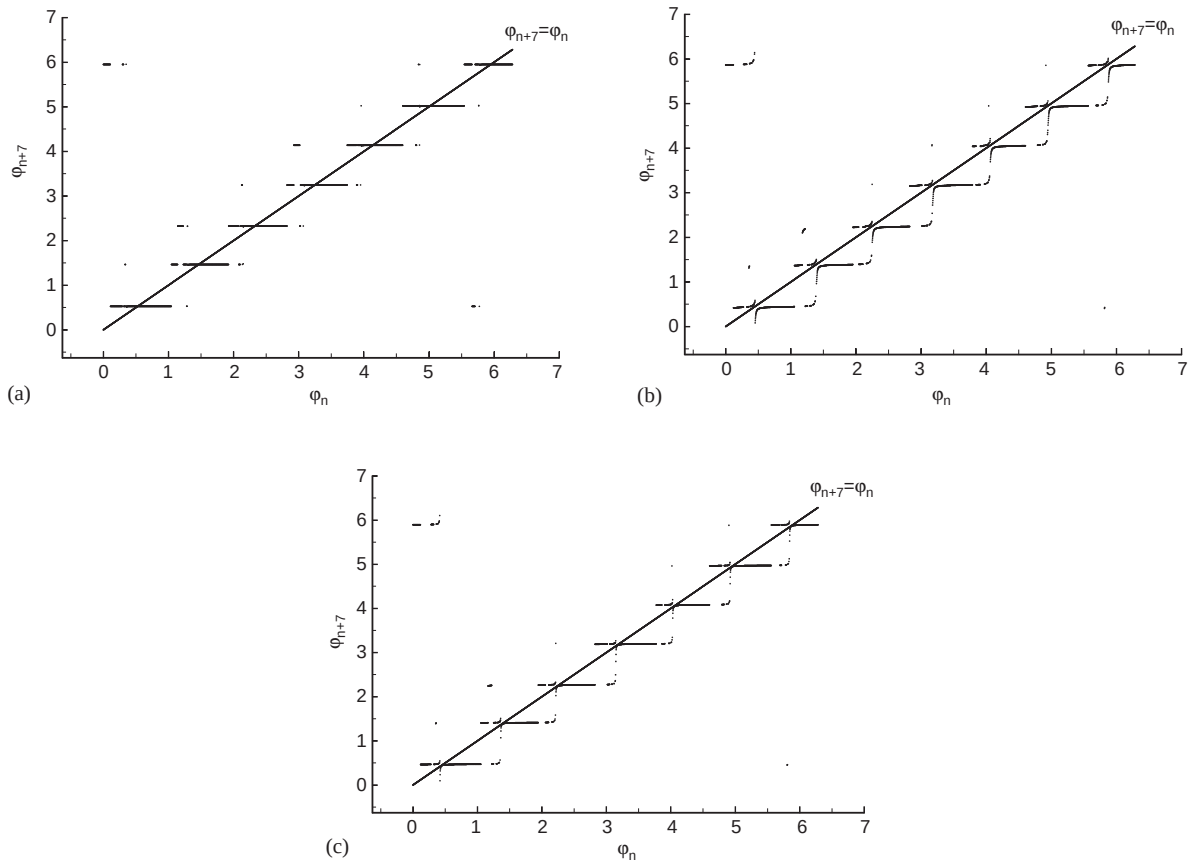

Fig. 5. Iterated maps with $M = 4, N = 7$: (a) $\varepsilon = 0.25$; (b) $\varepsilon = 0.20$; (c) $\varepsilon = 0.21$.

From bifurcation diagrams one can distinguish between periodic and non-periodic solutions, nevertheless, to judge whether a non-periodic solution is quasi-periodic or chaotic one needs other tools, among which are Poincaré sections and Lyapunov exponents. With their help it can be shown that both quasi-periodic and chaotic motions occur in the system. To illustrate, we choose two values of ε, 0.005 and 0.20, from the non-periodic bands in Fig. 4(c) and examine their corresponding Poincaré sections and Lyapunov exponents in Figs. 6(a)–(d). It is manifested that for ε equal to 0.005, the Poincaré section ($\varphi = 0$) is a closed curve and the corresponding Lyapunov exponent converges to zero with increasing number of iterations, and therefore the motion is quasi-periodic. For $\varepsilon = 0.20$, in contrast, the Poincaré section takes on an irregular pattern essentially dissimilar to the plots of finite number of points and of closed curves which correspond to periodic and quasi-periodic motions, respectively. Hence, the Poincaré section indicates chaos. In addition, the Lyapunov exponent converges to a positive number 0.03 along the increased number of iterates, which is one defining characteristic of chaos. Finally, Figs. 6(e) and (f) confirm the periodicity of the motion for $\varepsilon = 0.25$, in which the Poincaré section consists of one point and the Lyapunov exponent converges to a negative value of -0.92.

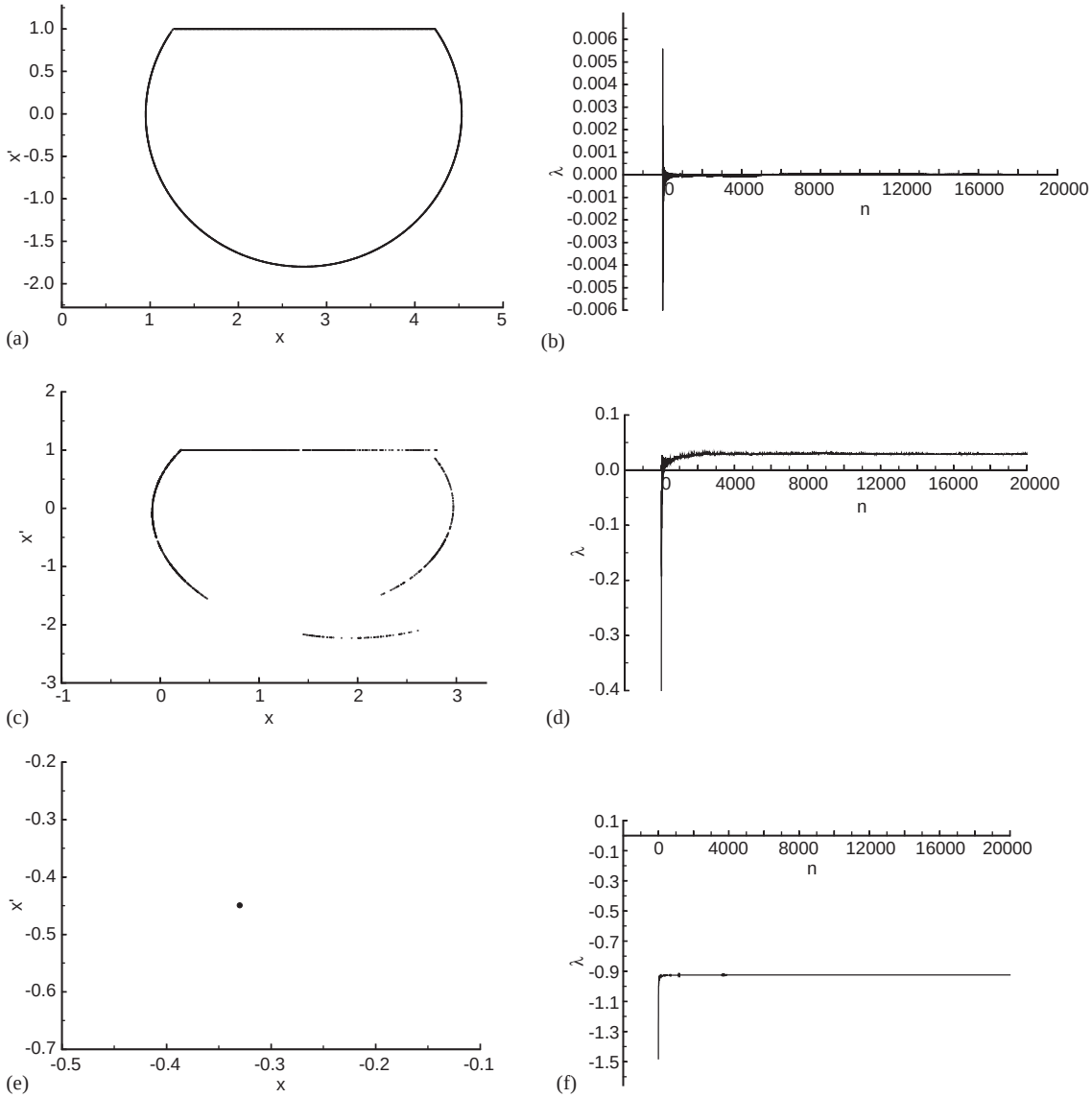

Fig. 6. (a), (c), (e) Poincaré sections and (b), (d), (f) Lyapunov exponents with $M = 1$ and $N = 4$: (a), (b) $\varepsilon = 0.005$; (c), (d) $\varepsilon = 0.20$; (e), (f) $\varepsilon = 0.25$.

In Fig. 7, the bifurcation diagrams for the cases of $M \geqslant N$ are shown. Fig. 7(a) illustrates the stick-to-slip transition displacement x vs. ε, with both M and N set to 1. Periodic, quasi-periodic and chaotic attractors are observed, which can be verified by the Poincaré sections for ε equal to 0.28, 0.15 and 0.24, respectively, as displayed in Figs. 8(a)–(c). More interestingly, there exists a parametric range, i.e. [0.18, 0.235], in which no point is plotted. This is a consequence of the fact that within the above parametric range the steady-state motion for the system is non-stick motion

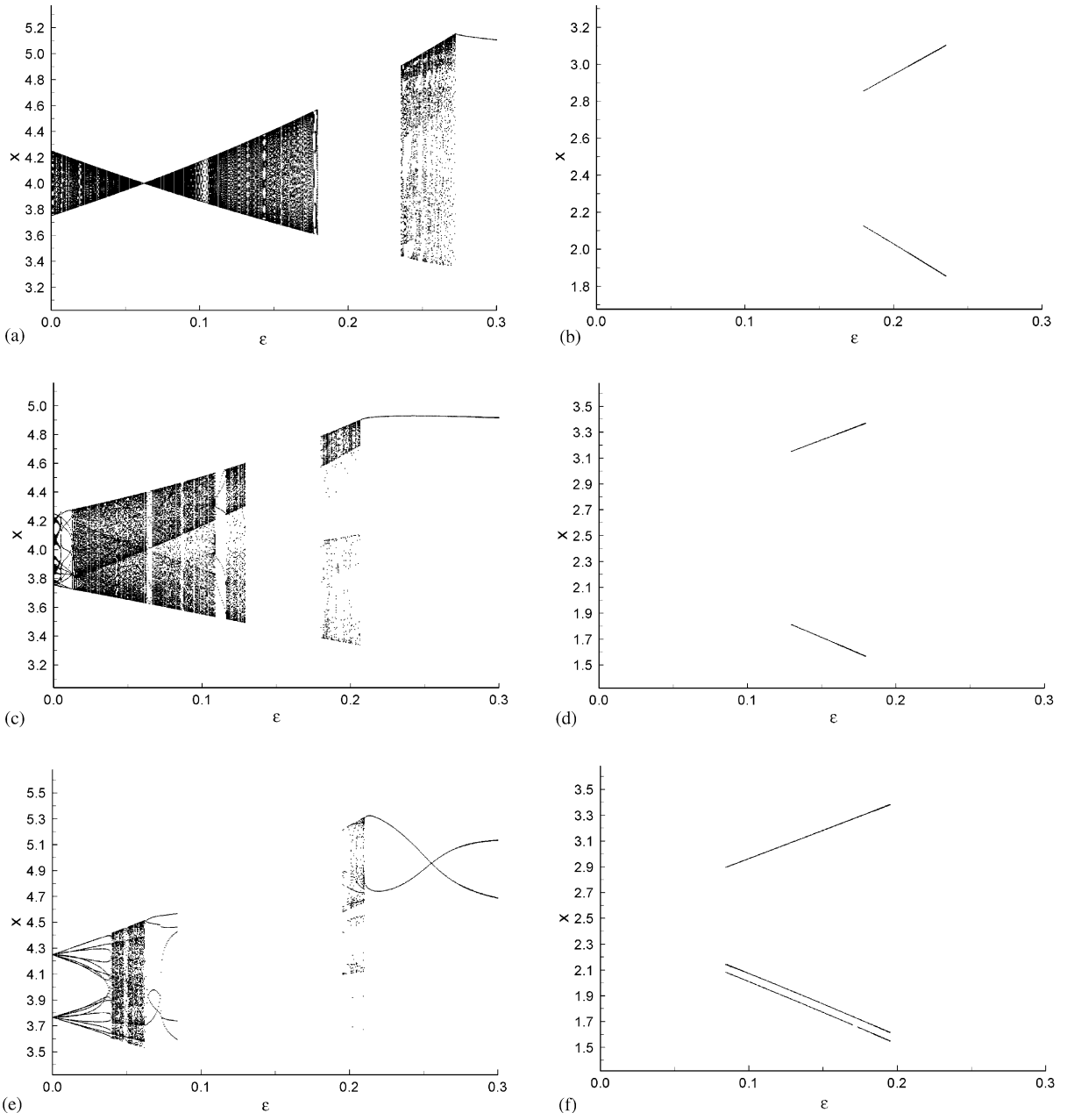

Fig. 7. Transition displacement x vs. ε with $M \geqslant N$: (a), (c), (e), (g) stick-slip motions and (b), (d), (f), (h) non-stick motions; (a), (b) $M = 1, N = 1$; (c), (d) $M = 3, N = 1$; (e), (f) $M = 9, N = 2$; (g), (h) $M = 8, N = 1$.

instead, where there is no stick-to-slip transition state. For the non-stick motion, we can plot bifurcation diagrams using the displacement of the mass when its velocity equals zero, as seen in Fig. 7(b). Obviously, the non-stick motion is periodic for the whole parametric range. Another

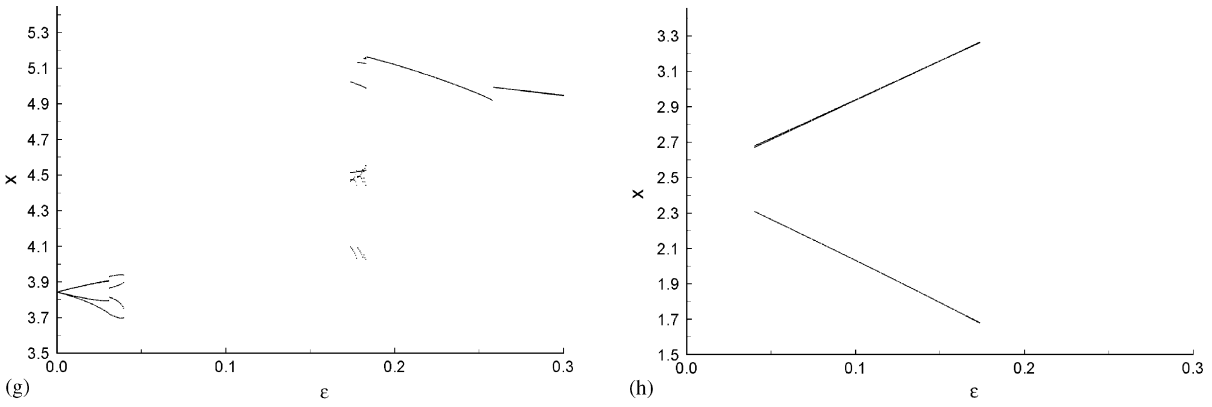

Fig. 7. (*Continued*)

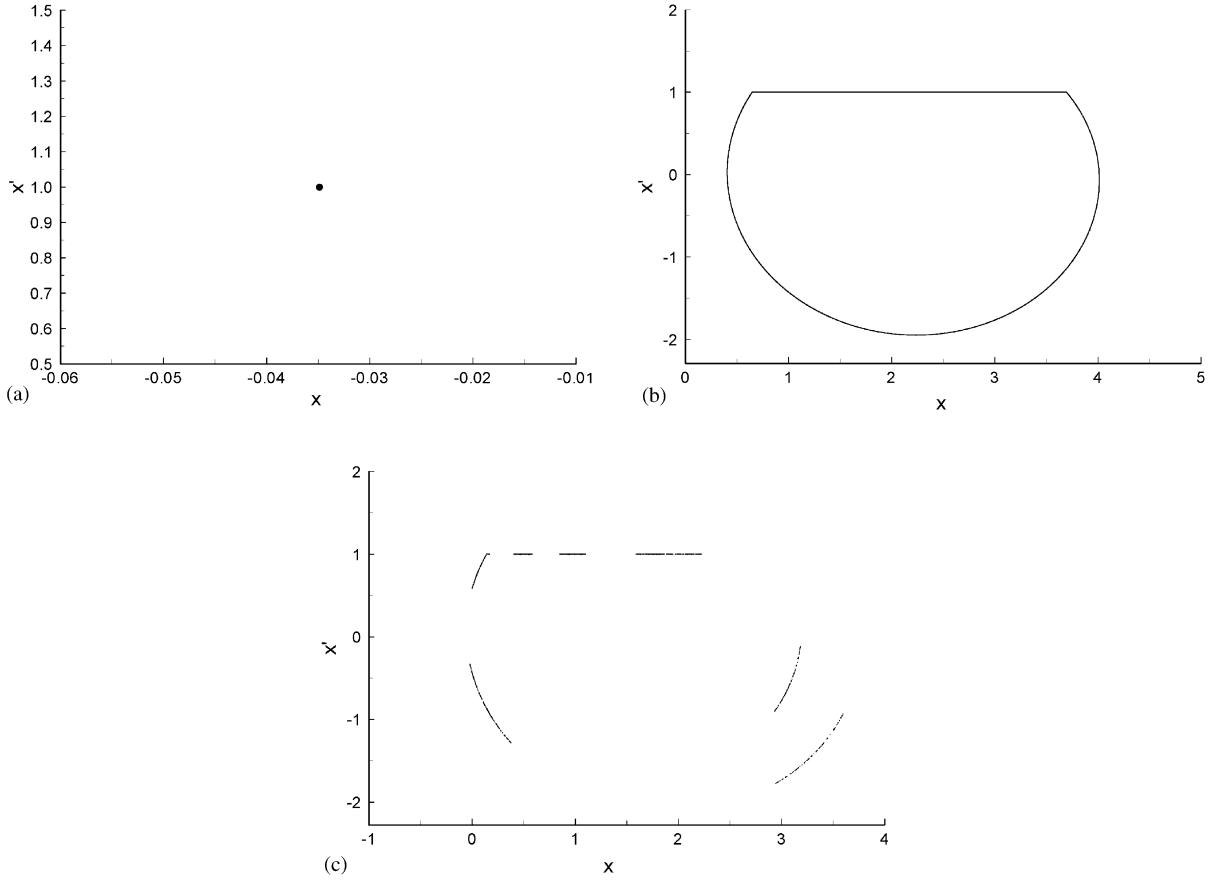

Fig. 8. Poincaré sections with $M = 1, N = 1$: (a) $\varepsilon = 0.28$; (b) $\varepsilon = 0.15$; (c) $\varepsilon = 0.24$.

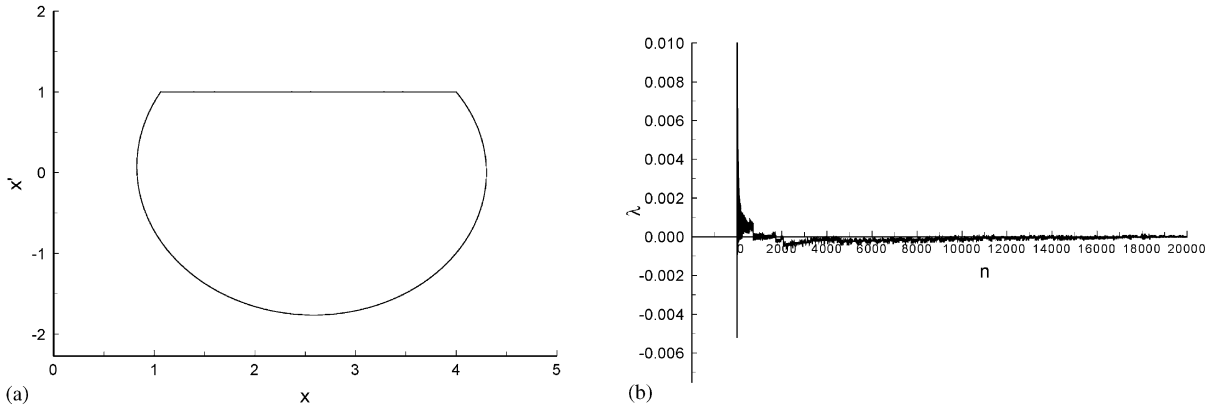

Fig. 9. (a) Poincaré section and (b) Lyapunov exponent with $M = 1, N = 1$ and $\varepsilon = 0.0625$.

phenomenon worth mention is that at $\varepsilon = 0.0625$ only one point is drawn in the bifurcation diagram Fig. 7(a), which may lead one to conclude that the corresponding response is periodic. In fact, though, the response of the system at that point is quasi-periodic, which can be verified with Figs. 9(a) and (b), where the corresponding Poincaré section is shown to be a closed curve and the Lyapunov exponent converges to zero. This unique phenomenon can be explained with the aid of Eq. (12). For quasi-periodic motions, the stick-to-slip transition displacement x_n in general varies with the phase angle φ_n, according to Eq. (12). With $\varepsilon = 0.0625$ and $M = N = 1$, however, Eq. (12) becomes an identical equation and consequently x_n always takes the value of 4. Thus, only one point, (0.0625, 4.0), is plotted in the bifurcation diagram although the motion is not periodic. Figs. 7(c–h) show the cases of M/N equal to 3/1, 9/2 and 8/1, respectively. It is evident that for all these cases of $M \geqslant N$, both types of steady-state motion, that is, stick-slip and non-stick motions, can take place, which is very different from the cases of $M < N$, where only stick-slip motions are observed. Moreover, it is found that all the non-stick motions are periodic, which implies that the stick phase plays a crucial role in the occurrence of non-periodic motions. Finally, a trend in the influence of M/N on the system dynamic behavior is discovered from these figures together with Figs. 7(a and b). It is observed that as M/N is increased from 1/1 to 8/1, less non-periodic motions occur and more periodic motions take place, with respect to the parameter ε. As a matter of fact, if M/N becomes big enough, such as 8/1, only periodic motions happen, as shown in Figs. 7(g and h).

5. Conclusions

The dynamics of a Coulomb friction damped block-on-belt system subjected to both parametric and external excitations has been studied. The emphasis is on examining the influence of the parametric excitation on the system dynamic behavior, under various frequency ratios between the external and parametric excitations, namely M/N. Numerical simulations show that the system possesses rich dynamics characterized by periodic, quasi-periodic and chaotic attractors, and also suggest the following conclusions only relevant to the attractors found in the simulations as other attractors may also exist in the system:

(1) A tangent bifurcation is identified in the bifurcation diagrams with the amplitude of the parametric excitation as bifurcation parameter, which gives rise to the transition from non-periodic motions to periodic motions for the system.
(2) When the excitation frequency ratio M/N is less than 1, only stick-slip motions occur regardless of the change of the parametric excitation amplitude. Besides, if the parametric excitation amplitude exceeds the a critical value which keeps the same despite the variation of the ratio M/N, only periodic solutions exist and they are of N-period.
(3) For cases of $M/N \geqslant 1$, in contrast, both stick-slip and non-stick motions can take place. It is also found that all the non-stick motions are periodic, indicating the crucial role of the stick phase in the occurrence of non-periodic motions. Moreover, as M/N is increased, less non-periodic motions occur whereas more periodic motions take place, with respect to the bifurcation parameter corresponding to the parametric excitation amplitude .

References

[1] J.P. Den Hartog, Forced vibrations with combined coulomb and viscous friction, *Transactions of the American Society of Mechanical Engineers* 53 (1931) 107–115.
[2] B.F. Feeny, F.C. Moon, Chaos in a forced oscillator with dry friction: experiments and numerical modeling, *Journal of Sound and Vibration* 170 (1994) 303–323.
[3] M. Oestreich, N. Hinrichs, K. Popp, Bifurcation and stability analysis for a non-smooth friction oscillator, *Archive of Applied Mechanics* 66 (1996) 301–314.
[4] U. Andreaus, P. Casini, Dynamics of friction oscillators excited by a moving base and/or driving force, *Journal of Sound and Vibration* 245 (2001) 685–699.
[5] B.L. Van De Vrande, D.H. Van Campen, A. De Kraker, An approximate analysis of dry-friction-induced stick-slip vibrations by a smoothing procedure, *Nonlinear Dynamics* 19 (1999) 157–169.
[6] U. Galvanetto, Dynamics of a three DOF mechanical system with dry friction, *Physics Letters A* 248 (1998) 57–66.
[7] U. Galvanetto, Some discontinuous bifurcations in a two-block stick-slip system, *Journal of Sound and Vibration* 248 (2001) 653–669.
[8] J.J. Thomsen, A. Fidlin, Analytical approximation for stick-slip vibration amplitudes, *International Journal of Non-Linear Mechanics* 38 (2003) 389–403.
[9] G. Cheng, J.W. Zu, Two-frequency oscillation with combined coulomb and viscous frictions, *Journal of Vibration and Acoustics* 124 (2002) 537–544.
[10] G. Cheng, J.W. Zu, Non-stick and stick-slip motion of a coulomb-damped belt drive system subjected to multi-frequency excitations, *Journal of Applied Mechanics* 70 (2003) 871–884.
[11] G. Cheng, J.W. Zu, Dynamics of a dry friction oscillator under two-frequency excitations, *Journal of Sound and Vibration* 275 (2004) 591–603.
[12] P. Casini, F. Vestroni, Nonstandard bifurcations in oscillators with multiple discontinuity boundaries, *Nonlinear Dynamics* 35 (2004) 41–59.
[13] A. Maccari, Multiple resonant or non-resonant parametric excitations for nonlinear oscillators, *Journal of Sound and Vibration* 242 (2001) 855–866.
[14] V.N. Belovodsky, The dynamics of a vibromachine with parametric excitation, *Journal of Sound and Vibration* 254 (2002) 897–910.
[15] A. Tondl, R. Nabergoj, The effect of parametric excitation on a self-excited three-mass system, *International Journal of Non-Linear Mechanics* 39 (2004) 821–832.
[16] R.C. Hilborn, *Chaos and Nonlinear Dynamics*, Oxford University Press, Oxford, 1994.